ICCAUA Proceedings Journal
Proceedings of the international conference of contemporary affairs in architecture and urbanism-ICCAUA
Volume 9 (December 2026), 2610254

Journal homepage: https://journal.iccaua.com/

DOI: https://doi.org/10.38027/ICCAUA2026EN0254

Passive Thermal Comfort and Energy Performance of Residential Morphologies in a Hot–Arid Climate: a Simulation-Based Assessment for Post-War Housing Reconstruction in Aleppo

*** [1] Mariam Altaema , [2] Sertaç Oruç**
[1, 2] Faculty of Natural Sciences and Engineering, Ankara Yıldırım Beyazıt University, Ankara, Türkiye
[1] E-mail: mariam.altaema24@aybu.edu.tr, [2] E-mail: sertacoruc@aybu.edu.tr
[1] ORCID: https://orcid.org/0000-0002-2761-557X , [2] ORCID: https://orcid.org/0000-0003-2906-0771

Received: 23.04.2026
Revised: 21.06.2026
Accepted: 01.07.2026
Available online: 10.07.2026

This article has been selected and peer-reviewed for publication in this journal as part of the 9th International Conference of Contemporary Affairs in Architecture and Urbanism, held on 7–8 May 2026 in Istanbul, Türkiye.

Abstract

Post-war housing reconstruction in Aleppo faces the dual challenge of delivering thermal comfort and improving thermal and energy performance under a hot-dry climate with constrained infrastructure. This study evaluates 24 residential morphologies across four plan families (L, U, Courtyard (box), and II) through dynamic free-running simulations in DesignBuilder, using current-climate weather data from Meteonorm for Aleppo. Annual mean operative temperature, PMV, PPD, discomfort hours, and heating and cooling energy demand were integrated through a Multi-Criteria Decision Selection (MCDS) weighted-sum model, prioritising operative temperature and discomfort hours (weight 0.25 each) alongside PMV, PPD, air temperature, heating demand, and cooling demand. L-type layouts demonstrated the strongest overall performance, with L27 ranked first overall, followed by L22, L18, and L13, while II27 ranked last (MCDS = 0.095). The study introduces a morphology-based decision-support framework integrating A/V ratio analysis, thermal comfort, energy performance, and MCDS ranking for post-war housing reconstruction in hot–arid climates.

Keywords: Thermal comfort; passive thermal performance; energy demand; residential morphology; courtyard housing; hot–arid climate; post-war reconstruction; building performance simulation; multi-criteria decision-making.

1. Introduction

Global temperatures are rising, with the Intergovernmental Panel on Climate Change (IPCC, 2021) projecting continued warming throughout the 21st century. The building sector is responsible for a large portion of final energy consumption globally (Lachheb et al., 2024), and climate change is fundamentally altering this consumption profile. Buildings are impacted directly, since keeping comfortable indoor conditions often demands more energy input (Jafarpur & Berardi, 2021; Roetzel et al., 2014). In future climate scenarios, it is expected that the demand for cooling energy in buildings will rise considerably, while comfort zones will become smaller in terms of space (Isinkaralar et al., 2024; Jafarpur & Berardi, 2021). In colder climates, the decrease in heating demand might somewhat balance out the rise in cooling needs; nonetheless, without adaptive strategies, overall energy use and thermal discomfort are expected to increase (Jafarpur & Berardi, 2021). Future projections further indicate that with the increasing frequency of heatwaves, cooling demand and peak electricity loads in buildings will increase significantly, while heating demand will decrease, but overall stress on energy grids will grow (Dirks et al., 2015; Jafarpur & Berardi, 2021).

In recent decades, the energy demand in the building sector, particularly for cooling and heating spaces, has increased significantly. This accelerating increase in energy consumption and environmental pollution in buildings (e.g., greenhouse gas emissions, etc.) is becoming a growing problem in many countries around the world (Lachheb et al., 2024). Future projections indicate that rising temperatures and more frequent heat waves—that is, rapid changes in climate characteristics as well as changes in the frequency and duration of intense weather events—will significantly increase the cooling demand and the risk of overheating in buildings (Dirks et al., 2015). Building insulation is being increased to reduce heating needs. This can directly reduce human thermal comfort. This problem may intensify with continued climate change. Along with these problems, environmental and economic sustainability are at risk (Ferdyn-Grygierek et al., 2021; Jafarpur & Berardi, 2021).

The intersection of climate change and post-war reconstruction constitutes one of the most complex urban planning and engineering challenges of the 21st century. Regional climate models, including the Coordinated Regional Climate Downscaling Experiment (CORDEX) and the Sixth Phase of the Coupled Model Inter-comparison Project (CMIP6), project pronounced warming across Syria alongside a shift toward greater aridity (Naaouf & Torma, 2023). These ensembles identify the Eastern Mediterranean and northern Syria, including Aleppo governorate, as a regional warming hotspot, with warming typically stronger over land than over the adjacent Mediterranean (Naaouf & Torma, 2023). Under

a high greenhouse gas concentration pathway (SSP5-8.5), mean annual near-surface temperatures over Syria have been reported as increasing up to approximately 6.4°C for 2080–2099 compared with 1995–2014 (Naaouf & Torma, 2023).
The relationship between rising outdoor temperatures and building energy consumption is non-linear and highly sensitive to the building envelope's thermal properties, internal gains, and occupant behavior. Simulation-based studies employing dynamic building-performance tools such as DesignBuilder have been widely used to assess the impacts of climate change on residential energy demand and thermal comfort (Aşıkoğlu Metehan et al., 2025; Escandón et al., 2023).
For Aleppo, where summer temperatures can exceed 40°C, cooling energy demand is expected to dominate annual loads as the climate warms. Reviews of building-energy impacts report that hot and arid regions can shift toward cooling-dominated demand profiles under warming, even where heating demand declines in milder winters (Iles et al., 2023; Kutty et al., 2024). In comparable Mediterranean and hot-climate studies, heating energy can decrease by tens of percent while cooling demand can rise substantially by mid- and late century under high-emission scenarios (Aşıkoğlu Metehan et al., 2025; Iles et al., 2023). Some analyses of heating and cooling load distributions report that historical heating-load ranges can exceed cooling ranges, while future projections reverse the relationship as cooling peaks increase with ambient temperature (Aşıkoğlu Metehan et al., 2025; Iles et al., 2023). A further concern is the overheating penalty: improved insulation that reduces winter heating loads can trap internal and solar heat gains in summer unless paired with appropriate shading and night ventilation (Dirks et al., 2015; Khaddour, 2024).
This change is particularly difficult in situations following conflict, where the electricity supply is unreliable. Increasing cooling degree days can lead to ongoing overheating and thermal discomfort when active cooling isn't accessible. In this context, thermal resilience refers to a building's capacity to maintain safe indoor temperatures during power outages, which may be more significant than traditional HVAC-based thermal comfort goals (Akande, 2010; Trepci & Rodriguez-Ubinas, 2025). Strategies that passively reduce solar gains and improve heat dissipation are essential for making spaces habitable again (Akande, 2010; Trepci & Rodriguez-Ubinas, 2025).
Passive design, also known as bioclimatic architecture, focuses on enhancing indoor environments by reducing heat gain and increasing heat dissipation through architectural and urban-form strategies instead of relying on mechanical systems (Akande, 2010; Trepci & Rodriguez-Ubinas, 2025). In Aleppo, this method can incorporate local features suited for hot and dry climates. Aleppo's traditional architecture has adapted to hot-arid climatic conditions for centuries with passive design strategies such as courtyard housing typologies, thick stone walls, and natural ventilation (Salkini, Greco, et al., 2017). However, the modernization process that began in the pre-war period and the urgent need for housing in the post-war period led to the abandonment of these passive strategies and the proliferation of climate-insensitive, energy-intensive reinforced concrete structures (Kousa et al., 2021).
Among vernacular elements, the mashrabia (carved wooden screen) is another important device. Traditionally used for privacy and daylight control, modern and kinetic variants are studied as shading devices that can reduce solar gains while preserving ventilation and daylight (Salkini, Swaid, et al., 2017; Trepci & Rodriguez-Ubinas, 2025). Strategic shading of south- and west-facing façades is especially important to mitigate late-afternoon heat gains (Trepci & Rodriguez-Ubinas, 2025; Zahiri & Altan, 2016).
A key challenge in reconstruction is the materials-performance gap. Conventional pre-war construction often used uninsulated masonry or concrete elements with high thermal transmittance (U-values). A study on the implementation of insulation code in Damascus reports large improvements in envelope U-values when compliant insulation is applied, with corresponding reductions in heating demand (Khaddour, 2024). However, in summer, insulation must be paired with shading and adequate nighttime ventilation to prevent heat buildup and elevated nighttime indoor temperatures (Khaddour, 2024). The literature confirms that the optimization of the building envelope and the integration of passive cooling techniques can significantly reduce energy consumption and carbon emissions in buildings in hot climates (Atmaca et al., 2021; Trepci & Rodriguez-Ubinas, 2025). Therefore, in the post-war resource-scarce environment, energy efficiency and thermal comfort have ceased to be a luxury and have become necessities for economic recovery and public health (Elshafei et al., 2022; Ghadanfar, 2021).
Beyond individual building components, the shape, orientation, and layout of a building all affect how well it ventilates and how hot or cold it gets. In hot-desert climates, building form significantly influences outdoor thermal comfort; for instance, circular building configurations were found to optimize wind velocity and pressure for natural ventilation, outperforming rectangular and U-shaped forms (Elshafei et al., 2022). The layout of streets and blocks in a city also shapes its microclimate. In dry and subtropical cities, streets running east-west with lower aspect ratios and well-placed open areas can modulate outdoor thermal conditions (Ben Ratmia et al., 2024; Ma et al., 2024; Tang et al., 2022).
This study assessed and compared the thermal performance of different building types in the context of post-war reconstruction in Aleppo. This study employs modern simulation methodologies to evaluate performance, rooted in indigenous cultural design principles. The study had 24 configurations, which were split into four groups based on shape: L-shaped, U-shaped, Courtyard (box), and II-type. The configurations were developed using different orientations, façade characteristics, and A/V ratios in accordance with the Syrian Building Code.
We used DesignBuilder version 6.1.7.007 to model the dynamic thermal systems and Meteonorm version 8.0 to determine the current weather conditions in Aleppo. The study extracted the following performance indicators: operative temperature, air temperature, Fanger PMV and PPD comfort indices, discomfort hours, and annual heating and cooling energy demand.

Despite growing literature on passive design in hot climates, several gaps remain. First, most comparative studies evaluate building morphologies using a single performance indicator (typically annual energy demand) rather than an integrated set of indoor comfort and moisture metrics. Second, studies specifically addressing post-war Syrian reconstruction from a simulation-based morphological perspective are scarce. Third, multi-criteria evaluation frameworks that explicitly account for the comfort-energy trade-off characteristic of hot-arid contexts are largely absent. The novelty of this study lies in integrating morphology-family comparison, area-to-volume (A/V) ratio optimization, thermal-comfort

assessment, and energy-performance evaluation within a single standards-based MCDS framework. Unlike previous studies that focused on isolated morphology types or single performance indicators, this research systematically compares 24 residential configurations across four morphology families using seven annual performance metrics under Aleppo's contemporary climatic conditions.

The present study addresses these gaps through the following contributions:

1. Systematic dynamic simulation of 24 residential configurations spanning four morphological families (L, U, box/courtyard, and II) and six area-to-volume ratios, using climate data representative of contemporary Aleppo.
2. Extraction of seven annual performance indicators capturing both comfort-oriented and energy-related dimensions of building performance.
3. Integration of these indicators through a transparent, standards-grounded MCDS weighted-sum framework that incorporates both thermal comfort metrics and heating and cooling energy demand.
4. Cross-family comparison and design-guidance synthesis oriented specifically toward the constraints and priorities of post-war reconstruction in Aleppo.
    a. Two research questions are addressed:
5. Which residential morphologies deliver the most robust indoor thermal comfort in Aleppo's current hot-arid climate, considering operative temperature, PMV/PPD, discomfort hours, and energy demand?
6. How can vernacular architectural principles—particularly courtyard typologies—be systematically integrated into evidence-based post-war reconstruction guidance?

The findings are intended to provide actionable design recommendations for architects, urban planners, and humanitarian engineering practitioners involved in the reconstruction of Aleppo.

2. Materials and Methods

The study employs a method that integrates simulation-based modeling, analysis of climatic data, and multi-criteria decision-making to evaluate the thermal performance of various building designs in the hot and dry conditions of Aleppo. The location is situated in central Aleppo, specifically at a latitude of 36.23°N and a longitude of 37.16°E. The climate is classified as hot-dry Mediterranean under the Köppen-Geiger classification (Peel et al., 2007; Beck et al., 2018). Hourly weather data for the simulation year was produced with Meteonorm v8.0 (Meteotest AG, 2021). This dataset encompasses global radiation, dry-bulb temperature, wind speed and direction, humidity, and diffuse radiation, recorded hourly throughout the year. Analysis of climate factors, including temperature variations, cooling and heating days, solar angles, and the distribution of solar radiation, was conducted to assist in the simulation setup and orientation planning. The methodology consists of four primary steps:

1. Climate data acquisition and pre-processing
2. Morphological design and parameterization of simulation models
3. Dynamic thermal simulation and output extraction
4. Multi-criteria (MCDM) performance evaluation.

2.1 Study area and climate data

Aleppo is located in northwestern Syria and has a hot, semi-arid Eastern Mediterranean climate, with extremely hot summers and cool, wet winters. Average annual rainfall ranges from about 330 mm in the city center to nearly 800 mm at higher elevations (Naaouf & Torma, 2023). Climate change is expected to intensify existing pressures on water availability, agriculture, and urban infrastructure; projections for 2050 indicate a potential 21% decrease in rainfall in the Euphrates and Aleppo Basin and temperature increases of up to 2.5°C (Alazzy et al., 2014).

In parallel, Aleppo's traditional architecture offers valuable passive-design strategies such as inner courtyards and passive cooling that are being reconsidered within bioclimatic housing models in the post-war reconstruction process. Recent reconstruction approaches increasingly emphasize integrating vernacular concepts with contemporary environmental practices to preserve cultural continuity and improve climate resilience (Salkini, Greco, et al., 2017; Chambers, 2022).

Hourly climate inputs were generated using Meteonorm (Meteotest AG, 2021), a stochastic weather data generator that integrates observations from the Global Energy Balance Archive (GEBA), the World Meteorological Organization (WMO) network, and the NOAA National Climate Data Center (Tootkaboni et al., 2021). Meteonorm produces Typical Meteorological Year (TMY) files for any geographic coordinate and can also generate future weather files based on global climate-model projections; these scenario datasets have been reported as reliable for mid- and late-century building-performance assessments (Escandón et al., 2023). Meteonorm has been benchmarked for solar-energy applications and used in PV and urban energy-demand modelling, supporting robust simulation through representation of inter-annual variability (Khatibi & Krauter, 2021; Pham et al., 2022; Delannoy et al., 2018; Tootkaboni et al., 2021). Outputs include an hourly series of solar radiation (global/diffuse/direct), ambient air temperature, relative humidity, wind, and precipitation.

2.2 Building Typologies and Configuration Design

We studied the four most common architectural styles in traditional Aleppo houses:

1. L-Form: Characterized by an open angle, this style allows sunlight in during winter and provides shaded areas in summer; it facilitates airflow when properly oriented.
2. U-Form: This design is open on one side, providing shaded areas in summer and retaining the sun's heat in winter; it also offers good ventilation when properly oriented.
3. Courtyard (box): (courtyard): Featuring a central enclosed courtyard, this style moderates temperatures year-round through natural ventilation and intermittent shading.
4. II-Form (double wing): Two parallel wings surrounding an inner courtyard.

The four plan families and their passive thermal strategies are illustrated in Figure 1.

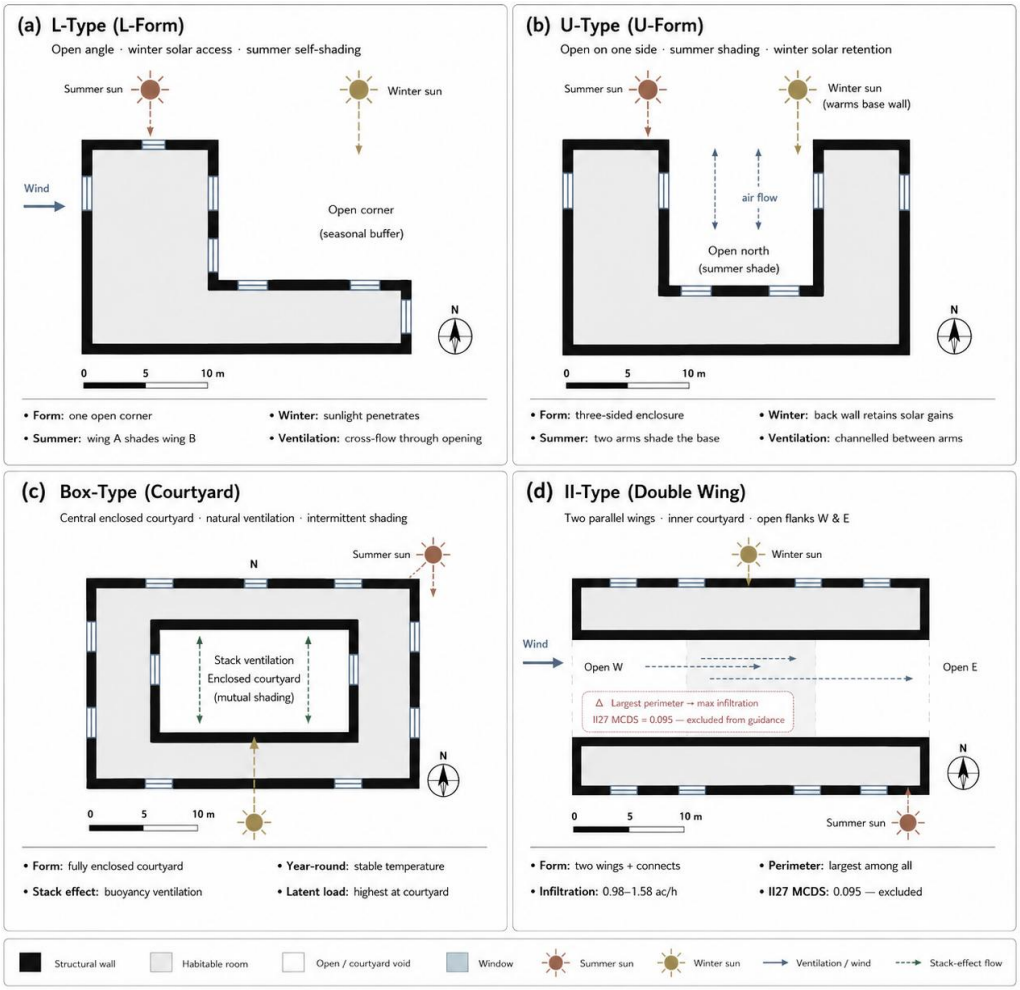

Figure 1. Four residential plan morphologies studied with passive thermal strategy annotation: L-Form (open corner), U-Form (open south), Courtyard (box) (central courtyard), and II-Form (double wing). All configurations are two storeys, 4.0 m floor height, with a courtyard facing glazing fraction of 30%.

A total of 24 alternatives were modelled in DesignBuilder (DesignBuilder Software Ltd., 2021) using different surface area-to-volume (A/V) ratios in increments of 0.10 across the range 0.50–1.00 m^{-1}, a key indicator of building form and its influence on thermal demand (Erdemir Kocagil & Koçlar Oral, 2015). A lower A/V ratio denotes a more compact building: as volume increases relative to exposed surface area, less envelope is exposed per unit of conditioned space, reducing heat exchange with the external environment. A higher A/V ratio indicates a more dispersed form with greater exposed envelope area per unit volume, increasing solar and conductive heat gains. Configuration labels combine the plan-family prefix with a number that increases with the A/V ratio (e.g., L10 denotes the L-type at A/V = 0.50 m^{-1} and L27 denotes the L-type at A/V = 1.00 m^{-1}). The resulting simulation matrix comprises 24 configurations (4 families × 6 A/V ratios), summarized in Figure 2.

Weather data for Aleppo were generated using Meteonorm to represent local station conditions, and building envelopes were modelled to match materials specified in the Syrian building code. Simulation outputs for each alternative were exported, aggregated, and evaluated through a multi-criteria decision process to identify the most suitable reconstruction options.

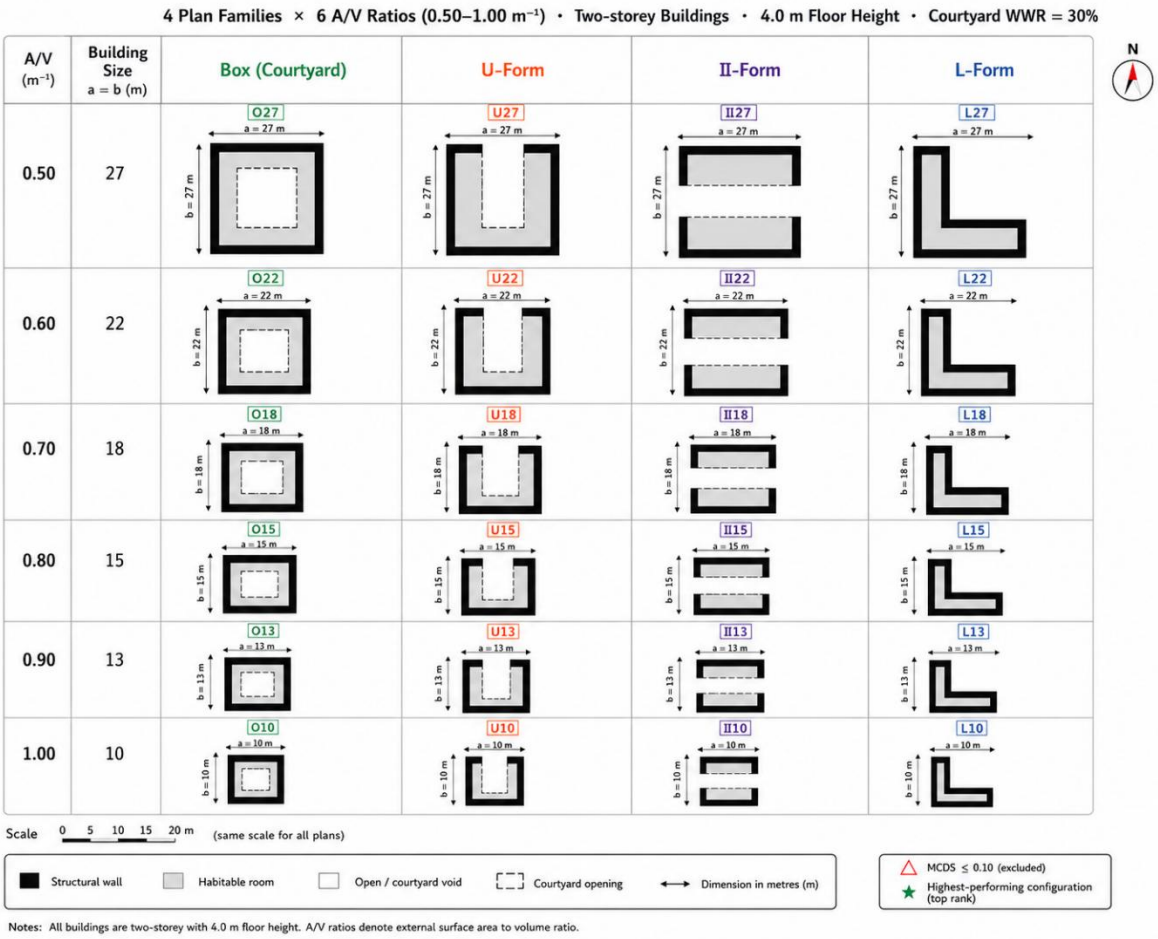

Figure 2. Simulation matrix — 24 residential configurations by plan family and A/V ratio.

2.3 Simulation Parameters and Boundary Conditions

All simulations used identical internal gain schedules, thermostat setpoints, and occupancy profiles to isolate the effect of building morphology. The Syrian Building Code envelope specification was applied uniformly: external walls of reinforced concrete with thermal insulation compliant with the national standard; a flat roof with an insulation layer; and double-glazed windows with a U-value of 2.8 W/m²K. Infiltration and natural ventilation were modelled using EnergyPlus's airflow network approach with crack coefficients appropriate for the construction type. Mechanical conditioning was not modelled; therefore, indoor thermal conditions reflect free-running (passive) operation, which is consistent with the post-war scenario in which a reliable electricity supply cannot be assumed. Heating and cooling demand values were reported as theoretical conditioning loads generated by the simulation engine for comparative evaluation purposes only.

Performance indicators were extracted as annual mean values over occupied hours (08:00–22:00), consistent with ASHRAE 55-2020 and ISO 7730:2005 protocols. Discomfort hours were defined as occupied hours in which the operative temperature falls outside the ISO 7730 Class B comfort envelope (±0.5 PMV). Annual heating demand and cooling demand were extracted in kWh per configuration, providing direct energy consumption indicators that quantify the active-conditioning effort required to maintain comfort beyond what the passive envelope can achieve. The simulation inputs—Syrian Building Code envelope specification, Meteonorm TMY climate file, and EnergyPlus airflow network—are consistent with those used in comparable validated studies of hot-arid residential buildings (Trepci & Rodriguez-Ubinas, 2025; Khaddour, 2024). Simulated annual mean operative temperatures (22.39–25.63°C) and PMV values (0.38–1.04) span the range expected for free-running residential buildings in Eastern Mediterranean summer conditions, with the anomalous II27 values reflecting the aerodynamic amplification effect documented in Section 3.4.

2.4 Multi-Criteria Decision Framework

To compare the 24 configurations in a transparent and reproducible manner and to integrate thermal comfort and energy-related indicators into a single ranking framework, this study employed a Multi-Criteria Decision Selection (MCDS) weighted-sum approach. The framework was conceptually informed by the principles of the Analytic Hierarchy Process (AHP) (Saaty, 1977, 1980), while maintaining a simplified weighted aggregation structure suitable for comparative building-performance evaluation. Criterion weights were established based on two complementary considerations: (i) internationally recognized thermal comfort standards, particularly ASHRAE Standard 55 (2020) and ISO 7730 (2005), and (ii) the reconstruction priorities of hot–arid, resource-constrained post-war contexts, where maintaining passive indoor comfort is prioritized over reducing operational energy demand alone.

Accordingly, operative temperature and discomfort hours received the highest weighting due to their direct relationship with habitability and thermal resilience under free-running conditions. PMV, PPD, and air temperature were included as supporting thermal-comfort indicators, while annual heating and cooling demand were assigned lower weights to

represent energy considerations without dominating the comfort-oriented evaluation. This weighting structure was adopted to provide a transparent and reproducible decision-support framework and does not represent an optimization procedure. The final weight distribution is presented in Table 1.

2.4.1 Criteria Selection and Weights

Seven criteria were selected to capture both comfort-oriented and energy-related dimensions of performance (Table 1). Criteria weights were established based on thermal-comfort priorities identified in ASHRAE 55 (2020), ISO 7730 (2005), and expert judgement according to two principles: (i) comfort priority—operative temperature and discomfort hours each receive the largest weight (0.25), reflecting the study's primary goal of habitable passive indoor conditions; PMV receives 0.10 as a complementary comfort index, PPD receives 0.15 as a direct occupant dissatisfaction outcome, and air temperature receives 0.10 as a physical driver; and (ii) energy indicators—annual heating demand and cooling demand each receive a weight of 0.075, reflecting their importance in the resource-constrained post-war context without overshadowing the comfort criteria. Weights sum to 1.0.

Table 1: Multi-criteria weights in the MCDS model.

Criterion	Weight
Air Temperature (°C)	0.10
Operative Temperature (°C)	0.25
Annual Heating Demand (kWh)	0.075
Fanger PPD (%)	0.15
Discomfort hrs (all clothing) (hrs)	0.25
Fanger PMV (–)	0.10
Annual Cooling Demand (kWh)	0.075
Total	1.0

2.4.2 Normalization of indicators

Because the criteria have different units and ranges, each raw indicator xij is transformed into a normalised score sij in the range $s_{ij} \in [0, 1]$ using min–max normalization across the 24 configurations.

Lower-is-better criteria (air temperature, operative temperature, PPD, discomfort hours, heating demand, cooling demand):

$$s_{ij} = \frac{x_{max} - x_{ij}}{x_{max} - x_{min}}$$

where x_max and x_min are the maximum and minimum values of the criterion across all configurations.

Higher-is-better criteria (not used in this study unless explicitly stated):

$$s_{ij} = \frac{x_{ij} - x_{min}}{x_{max} - x_{min}}$$

Target-based criteria (PMV, target t = 0):

$$d_{ij} = |PMV_{ij} - t|$$

$$s_{ij} = \frac{d_{max} - d_{ij}}{d_{max} - d_{min}}$$

where d_max and d_min are computed across all configurations.

This assigns scores near 1 to configurations closest to thermal neutrality and near 0 to the most deviating cases.
This normalization places all criteria on a comparable [0,1] scale while preserving relative differences between alternatives.

2.4.3 Weighted-Sum Aggregation and Sensitivity

For each configuration j, the overall MCDS score is computed using a weighted-sum model:

$$Score_j = \sum_i (w_i \times s_{ij})$$

where wi is the normalised weight of criterion i and $\sum i\ wi = 1$.

Configurations with higher composite scores exhibit better integrated performance under the adopted weights. The framework is transparent in that any single criterion's contribution is directly proportional to its weight, and alternative weighting assumptions can be readily evaluated. Future work should include a formal sensitivity analysis to assess the stability of rankings under varied weighting schemes.

Following this, we synthesized the findings to determine the most efficient and comfortable building configuration and presented recommendations for design strategies and future research directions. The research methodology is illustrated in Figure 3.

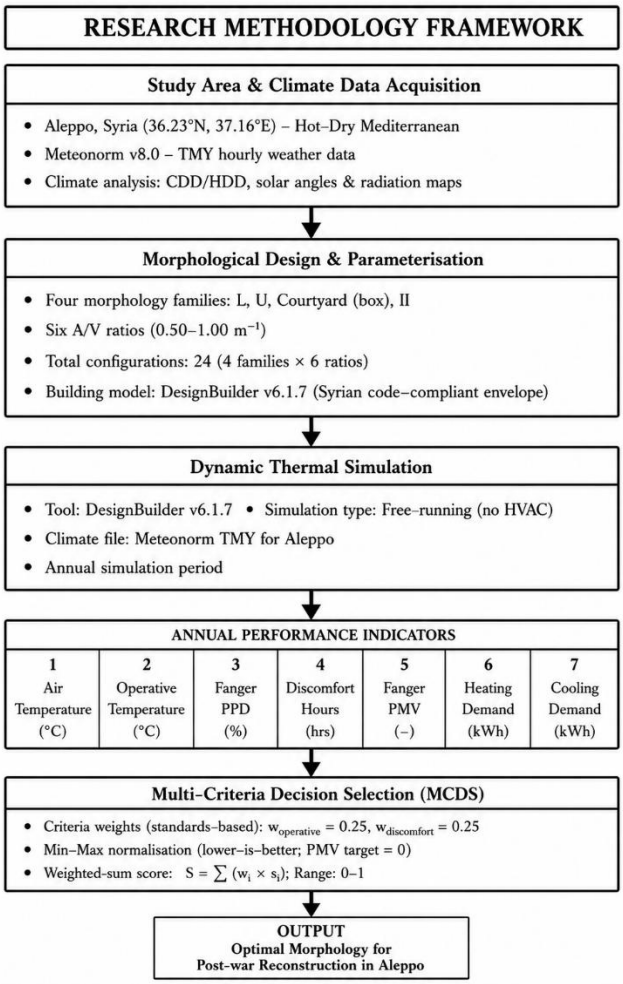

Figure 3. Research Methodology Framework (Developed by the Authors).

The methodological novelty of this research lies in combining parametric morphology analysis, dynamic thermal simulation, and weighted multi-criteria decision selection within a unified framework capable of ranking residential design alternatives according to both comfort and energy-performance objectives.

3. Results

This section presents a simulation analysis of all studied configurations using DesignBuilder software, followed by an evaluation of Multi-Criteria Decision Selection (MCDS). Subsections analyze each design group within a single family. The next stage provides a summary of the overall comparison between the four groups. Finally, the results are presented within the broader context of studies on passive house design in hot, arid regions, particularly in post-disaster and post-war settings.

The area-to-volume (A/V) ratio is a common engineering metric that directly impacts the thermal performance of passive house designs. It expresses the proportion of exposed envelope area relative to conditioned volume: a lower A/V ratio indicates a more compact building with less surface exposed per unit of interior space, while a higher A/V ratio indicates a more dispersed form with greater envelope exposure. Higher A/V ratios, therefore, lead to increased solar heat gain in summer and greater conductive and convective heat exchange with the external environment, resulting in greater thermal stress for occupants in the absence of mechanical conditioning. This relationship is further shaped by each family's geometric organisation: at a given A/V ratio, different plan families distribute their outer envelope differently, affecting mutual shading, natural ventilation pathways, and the proportion of interior courtyard to exterior surface.

3.1 L-type configurations (L10, L13, L15, L18, L22, L27)

L-shaped configuration structure with one side open. This design allows for better sun penetration in winter while ensuring shaded areas during summer. The open side can help facilitate airflow, depending on its orientation, as shown in Figure 4. Table 2 summarises annual mean indoor conditions, comfort indices, and energy demand indicators for the six L-type configurations.

Table 2: Performance indicators for L-type residential configurations in Aleppo.

Configuration	Air Temp (°C)	Operative Temp (°C)	Heating Demand (kWh)	PPD (%)	Discomfort Hours (hrs)	PMV	Cooling Demand (kWh)	Solar Gains (kWh)
L10	22.37	23.04	178	23.27	181	0.574	146	2380
L18	22.37	22.73	146	19.44	149	0.453	121	2350
L15	22.55	22.94	152	20.63	154	0.495	126	2375
L22	22.28	22.65	146	19.04	145	0.439	117	2335
L13	22.49	22.83	144	19.77	147	0.467	118	2360
L27	22.05	22.39	131	17.11	133	0.379	104	2310

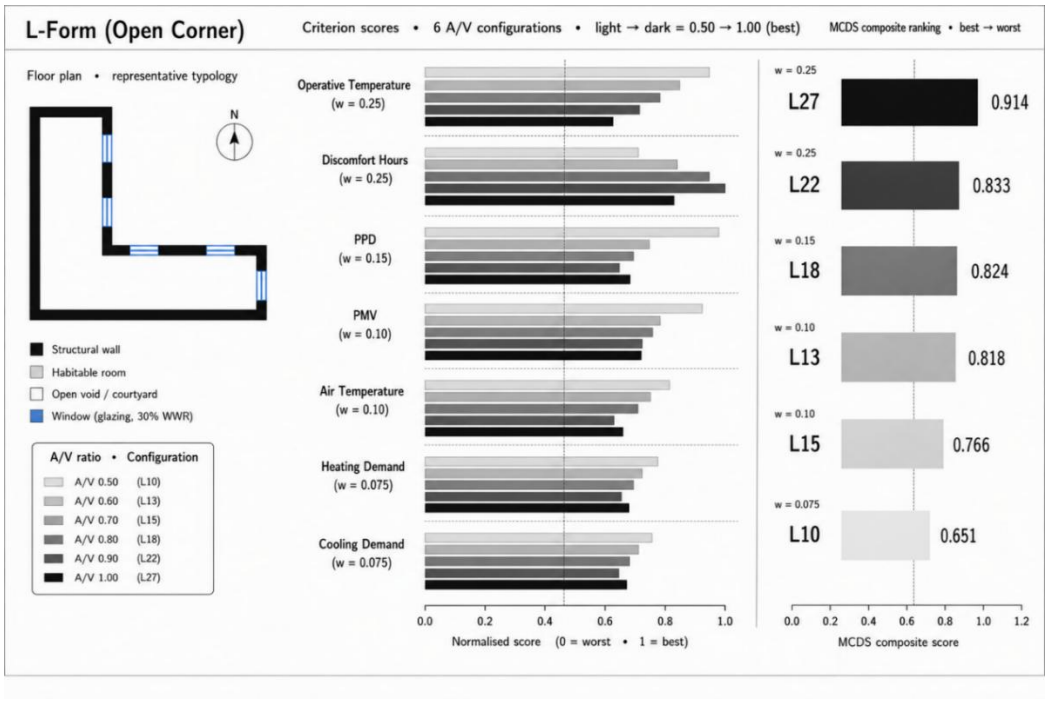

Figure 4. L-Form (Open Corner): normalized criterion scores and MCDS ranking for six configurations. ★ L27 achieved the highest composite score (0.914). (Developed by the Authors).

The average annual air temperature for group (L) ranged between 22.05 and 22.55°C, while operative temperature ranged between 22.39°C (L27) and 23.04°C (L10). These results reflect the hot-arid climate of Aleppo, in which operative temperature and discomfort duration constituted the principal differentiating comfort indicators across L-type configurations.

L27 demonstrated the strongest overall thermal-comfort performance within the group. It recorded the lowest PMV value (0.38, indicating the closest approach to thermal neutrality), the lowest PPD (17.11%), and the lowest operative temperature in the group (22.39°C). These results indicate that geometric organization, self-shading, orientation, and airflow distribution play a significant role in passive thermal behavior. In the L-type family, the open-angle geometry appears to offset some of the thermal penalties typically associated with increased exposed-envelope ratios in hot–arid climates. L27's comparatively low heating and cooling demand (131 kWh and 104 kWh, respectively) further confirms its suitability as the leading morphology for resource-constrained post-war reconstruction.

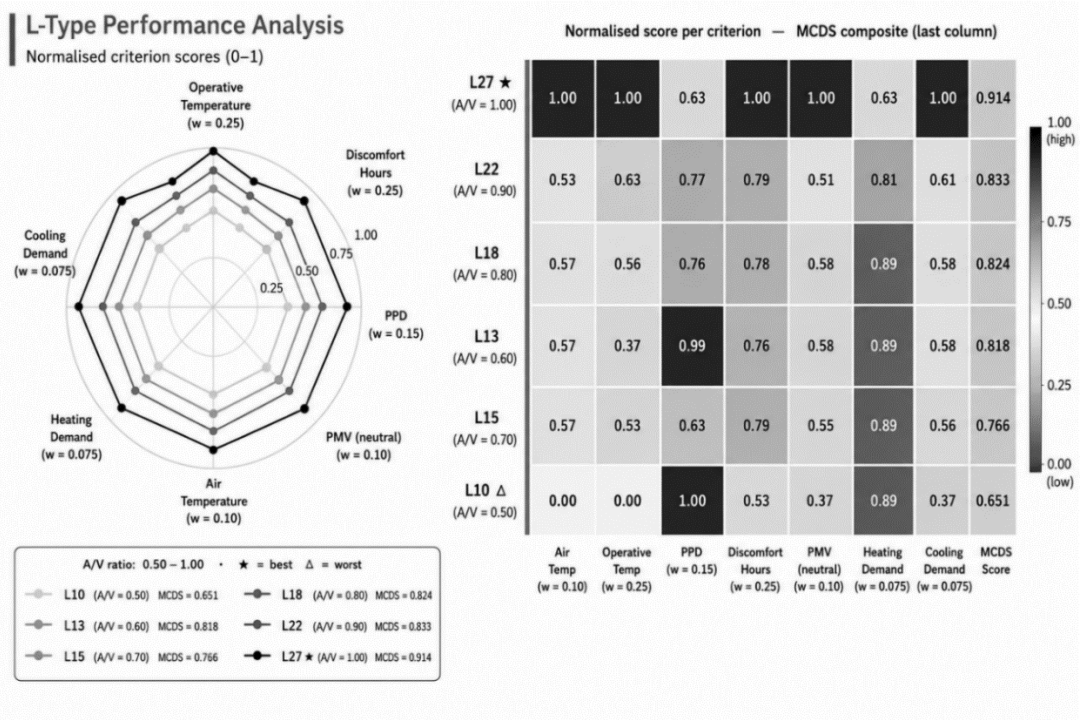

Figure 5. Radar chart and normalized score heatmap for L-type configurations. L27 achieved the highest composite performance score. (Developed by the Authors).

L22 and L18 achieved moderate energy demands (cooling: 117 and 121 kWh, respectively) together with good comfort levels (PPD 19.04% and 19.44%, 145 and 149 discomfort hours, and PMV 0.439 and 0.453, respectively).
The L15 configuration exhibited relatively lower comfort performance, with a PPD of 20.63% and 154 discomfort hours, although it maintained a moderate cooling demand of 126 kWh. L13 maintained comparatively good thermal performance (PPD 19.77%, 147 discomfort hours) with moderate cooling demand (118 kWh), while L27 recorded the lowest cooling demand in the family (104 kWh), further reinforcing its superior overall passive thermal performance.
L10 demonstrated the weakest performance in the group, with the highest PMV (0.574), the highest PPD (23.27%), and the longest discomfort period (181 hours). It also recorded the highest operative temperature (23.04°C). This behavior suggests that more dispersed geometries with increased exposed-envelope area reduce the effectiveness of passive thermal regulation in hot–arid climates. The comparative performance patterns are illustrated in Figure 5.

3.2 U-type configurations (U10, U13, U15, U18, U22, U27)

U-type Plan: U-shaped design with an open courtyard on one side. This configuration can trap heat in winter and, if oriented correctly, can provide shade and coolness during summer, as shown in Figure 6.
Table 3 summarises annual mean indoor conditions, comfort indices, and energy demand indicators for the six U-type configurations.

Table 3: Performance indicators for U-type residential configurations in Aleppo.

Configuration	Air Temp (°C)	Operative Temp (°C)	Heating Demand (kWh)	PPD (%)	Discomfort Hours (hrs)	PMV	Cooling Demand (kWh)	Solar Gains (kWh)
U10	22.08	22.02	464	19.49	148	0.541	739	2390
U15	22.07	22.03	522	19.51	163	0.538	1202	2354
U13	22.19	22.15	541	19.42	149	0.552	947	2424
U18	22.13	22.09	525	19.48	161	0.543	1207	2387
U22	22.11	22.08	554	19.48	166	0.537	1516	2419
U27	22.12	22.10	604	19.41	166	0.491	1977	2475

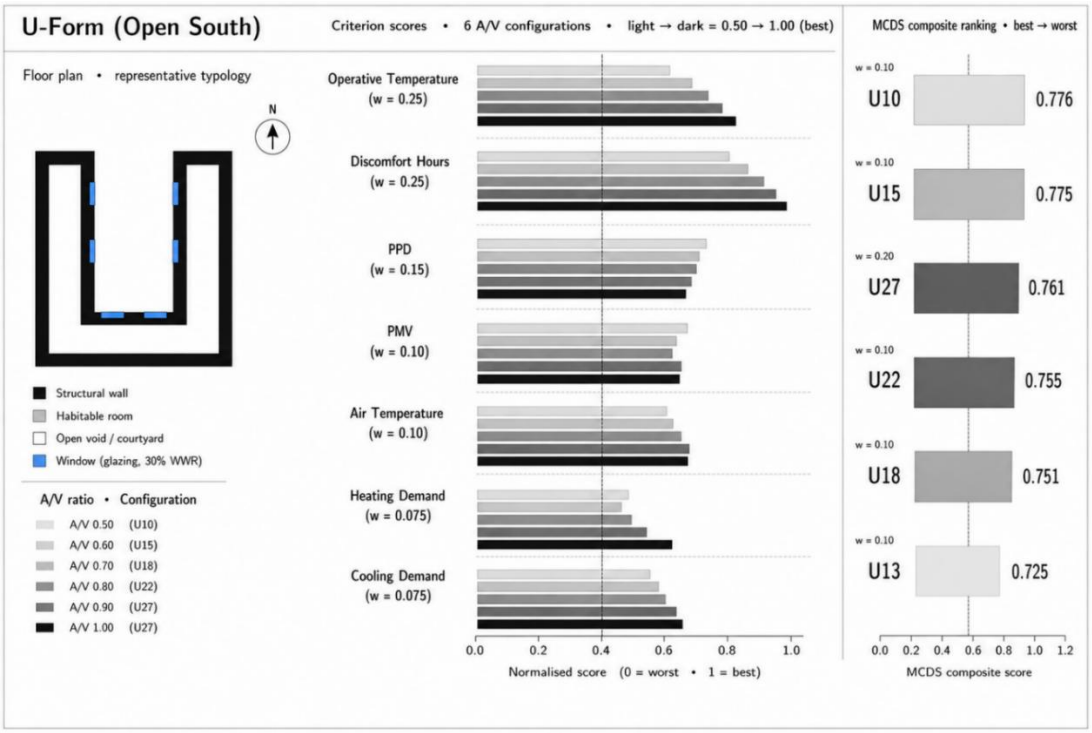

Figure 6. U-Form (Open South): normalized criterion scores and MCDS ranking for six configurations. U10 ranked first (MCDS = 0.848). (Developed by the Authors).

When analyzing the group of U-shaped configurations, we find that thermal comfort did not reach the optimal level, as the PMV values were all positive, ranging from 0.535 to 0.552 across all six U-type configurations. A gradual improvement was observed from U10 to U27, although PMV values remained within a narrow warm-comfort range (0.535–0.552) across the entire family. Considering the percentage of dissatisfied customers, PPD ranged from 19.41% (U27) to 19.51% (U15), a very narrow band indicating comparable occupant dissatisfaction across the family.

A gradual reduction in operative temperature and perceived thermal stress was observed across the family, resulting in a slight reduction in perceived heat and improved PMV and PPD values. Discomfort hours ranged from 148 (U10) to 166 (U22 and U27), reflecting limited variation in occupant dissatisfaction across the family despite large differences in cooling demand. The operative temperature remained nearly constant across all six configurations (22.02–22.15°C), confirming that the U-type geometry's open courtyard effectively moderates indoor temperature regardless of A/V ratio.

U10 achieved the best composite MCDS score in the family (0.848), combining the lowest operative temperature (22.02°C) with the lowest cooling demand (739 kWh). U13 (0.813) followed closely. U27, while achieving the second-lowest operative temperature (22.10°C) and best PMV/PPD values, ranked lower overall due to its very high cooling demand (1,977 kWh). The results are shown in Figure 7.

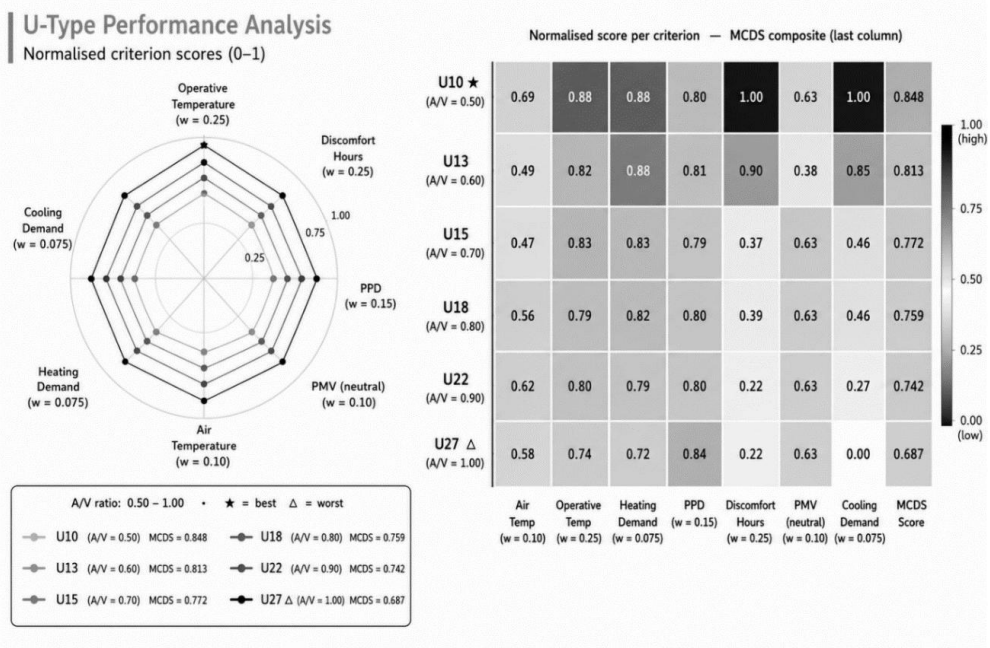

Figure 7. Radar chart and normalised score heatmap for U-type configurations. Cooling demand increases with A/V ratio across the U family, while operative temperature and PMV remain comparatively stable. (Developed by the Authors).

3.3 Courtyard (box) configurations (box10, box13, box15, box18, box22, box27)

Courtyard (box) (Central Courtyard): This design features a courtyard at the center of the building, ensuring even distribution of light and air. In winter, the central location can help retain heat by minimizing exposure to external cold. During summer, it can facilitate airflow and provide shade, as shown in Figure 8.

Table 4 summarises annual mean indoor conditions, comfort indices, and energy demand indicators for the six courtyard (box) configurations.

Table 4: Performance indicators for courtyard (box) configurations in Aleppo.

Configuration	Air Temp (°C)	Operative Temp (°C)	Heating Demand (kWh)	PPD (%)	Discomfort Hours (hrs)	PMV	Cooling Demand (kWh)	Solar Gains (kWh)
box10	22.52	23.20	620	23.83	200	0.510	1800	2480
box13	22.19	22.75	575	20.99	174	0.420	1500	2435
box15	22.38	22.94	590	19.24	145	0.448	1650	2450
box18	22.22	22.83	605	20.52	168	0.433	1720	2460
box22	22.21	22.81	615	20.27	164	0.428	1760	2470
box27	22.05	22.58	635	18.28	148	0.381	1850	2495

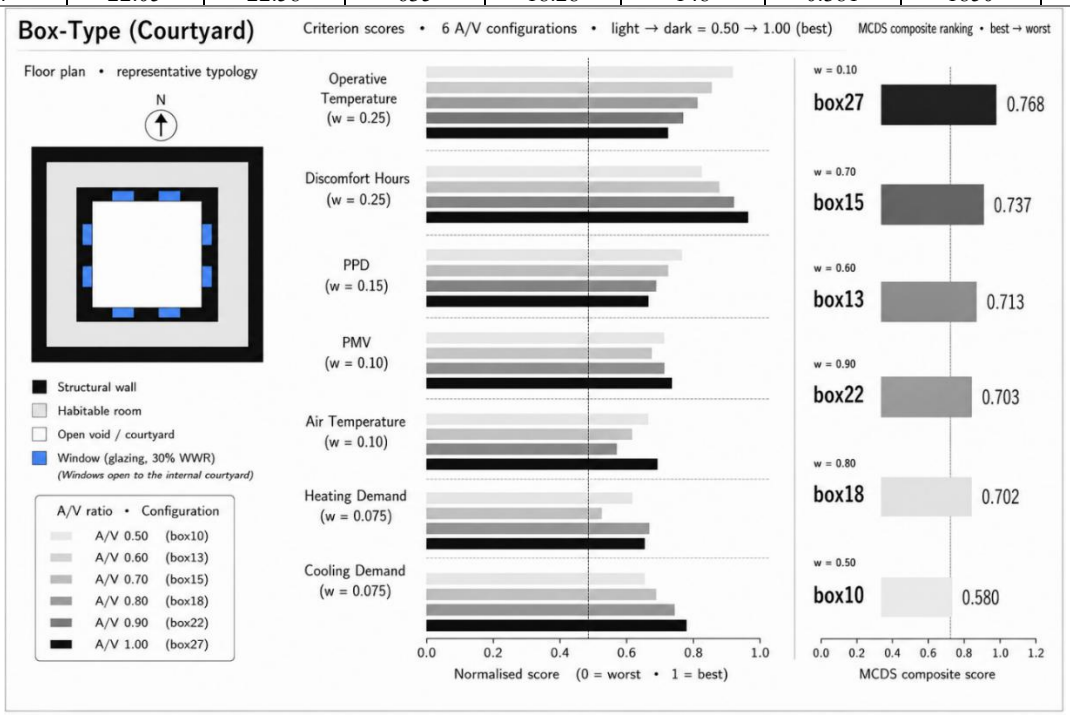

Figure 8. Courtyard (Box-Type): normalized criterion scores and MCDS ranking for six configurations. Box27 achieved the highest composite score (MCDS = 0.775). (Developed by the Authors).

In the box configurations, air temperatures ranged from 22.05 to 22.52°C, and operative temperatures ranged from 22.58 to 23.20°C.

Box 27 exhibited the best thermal performance, recording the lowest PPD (18.28%) and PMV (0.381) values and the fewest hours of thermal discomfort (148 hours). Conversely, Box 10 demonstrated the worst thermal performance across all comfort indicators. Box15 represented a comparatively balanced configuration, recording the lowest discomfort duration (145 h) while maintaining moderate performance across the remaining indicators.

Cooling demand across the box family remained consistently high, ranging from 1,500 kWh (Box13) to 1,850 kWh (Box27). a narrower range than in U-type or II-type configurations, reflecting the enclosed courtyard's moderating effect on solar penetration.

Overall, Box 27 performed best, followed by Boxes 15 and 13. Box 10 ranked last within its family due to the highest operative temperature (23.20°C) and the most discomfort hours (200). The results are shown in Figure 9.

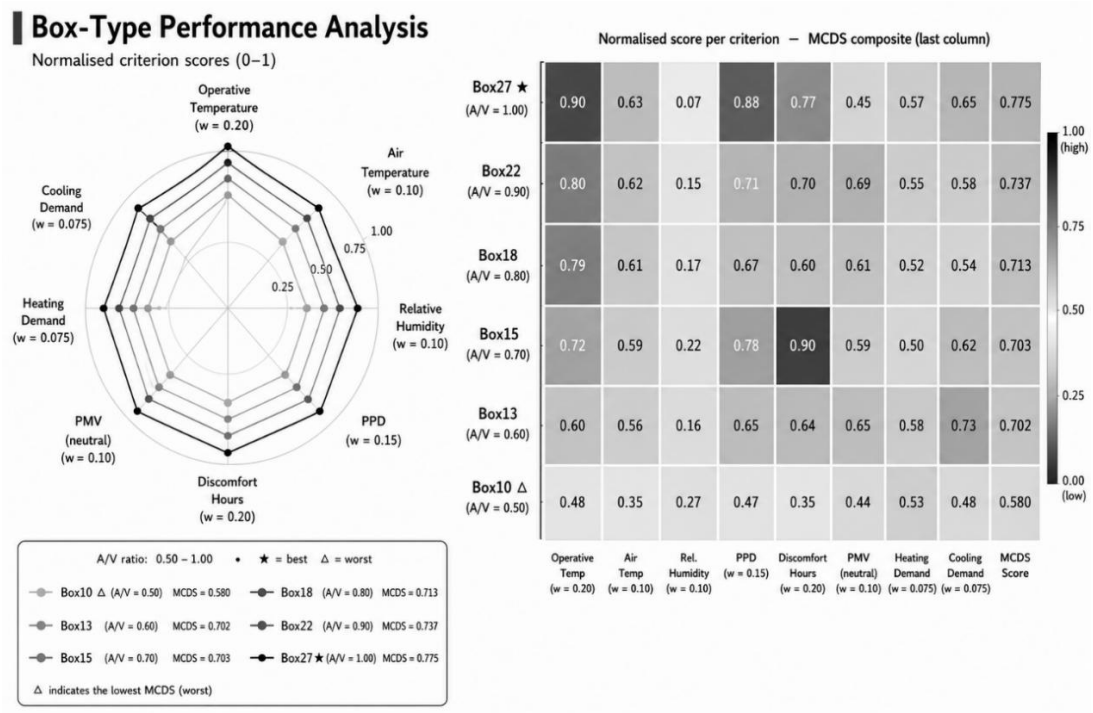

Figure 9. Radar chart and normalised score heatmap for Courtyard (box) configurations. The enclosed morphology delivers competitive comfort performance across all A/V ratios, though cooling demand is substantially higher than in L-type configurations. (Developed by the Authors).

3.4 II-type configurations (II10, II13, II15, II18, II22, II27)

The double-wing II-Form: This design seems to focus on providing an inner sanctum or space, probably shielded from external factors. In winter, this design might help in insulating the interior from cold, and during summer, it can act as a cool retreat, as shown in Figure 10.

Table 5 summarises the II-type configurations, which combine two intersecting wings around inner courts.

Table 5: Performance indicators for II-type residential configurations in Aleppo.

Configuration	Air Temp (°C)	Operative Temp (°C)	Heating Demand (kWh)	PPD (%)	Discomfort Hours (hrs)	PMV	Cooling Demand (kWh)	Solar Gains (kWh)
II10	22.40	23.02	505	22.47	183	0.474	1030	2410
II13	22.37	23.01	519	22.00	181	0.472	1045	2435
II15	22.45	23.18	540	23.00	189	0.504	1100	2442
II22	22.33	23.13	554	20.22	163	0.465	1516	2419
II18	22.22	22.83	498	20.73	175	0.436	950	2398
II27	24.75	25.63	610	44.59	236	1.040	2150	2550

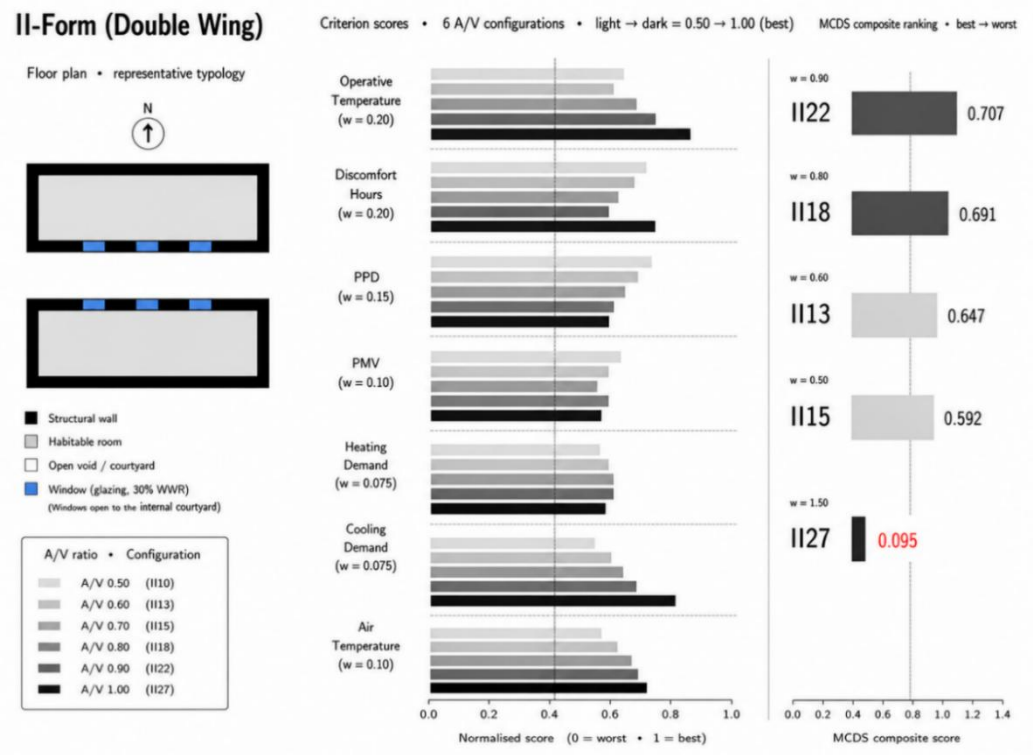

Figure 10. II-Form (Double Wing): normalized criterion scores and MCDS ranking for six configurations. △ II27 recorded the lowest composite score (MCDS = 0.095). (Developed by the Authors).

Within the II family, air temperature ranged from 22.22°C (II18) to 24.75°C (II27), and operative temperature from 22.83°C to 25.63°C. II18 demonstrated the best comfort performance in the family, with an operative temperature of 22.83°C, PMV of 0.44, PPD of 20.73%, and 175 discomfort hours. II22 offered a moderate balance with 163 discomfort hours and PMV of 0.46. II27 exhibited severe overheating: operative temperature 25.63°C, PMV 1.04 (the only configuration in the study to reach the ASHRAE "Hot" threshold), PPD 44.59%, and 236 discomfort hours. Based on the composite MCDS evaluation, II18 achieved the highest score within the II family.

II27 exhibited the worst performance in the study overall, scoring 0.095 on the MCDS framework. Its extreme operative temperature (25.63°C), PMV (1.04), PPD (44.59%), and 236 annual discomfort hours collectively indicate severe overheating under passive operation. The analysis is shown in Figure 11.

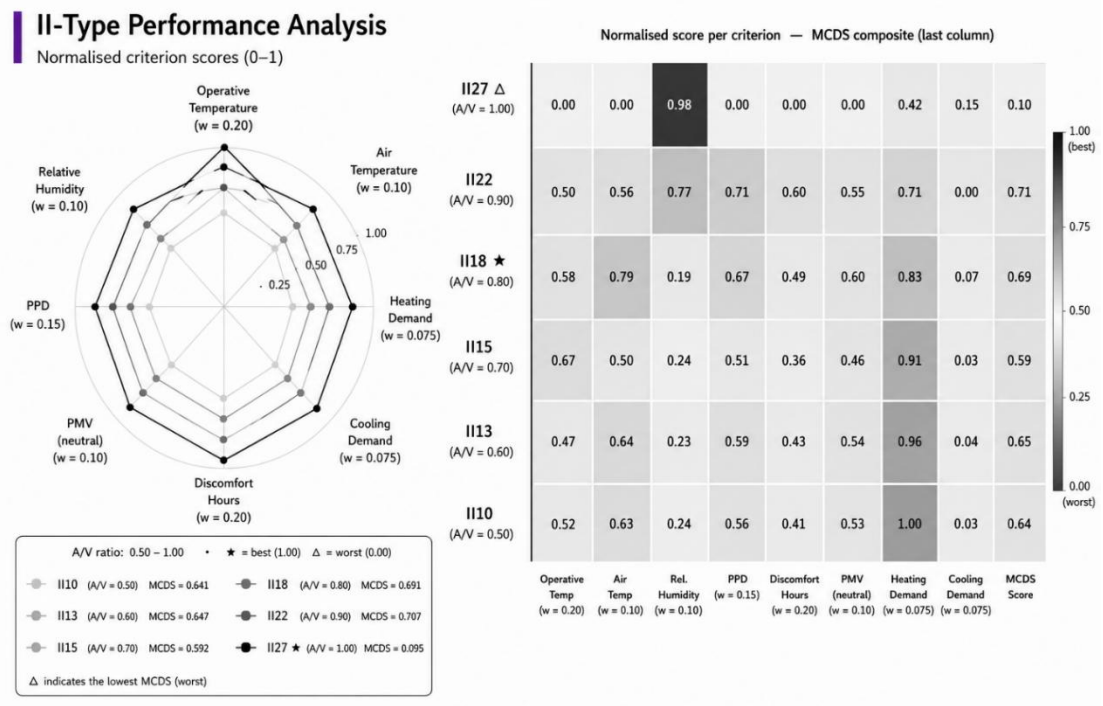

Figure 11. Radar chart and normalized score heatmap for II-type configurations. II27 (△) collapses on all comfort criteria, representing the worst-performing configuration across the entire study. (Developed by the Authors).

3.5 Multi-Criteria Ranking across All Configurations

A multi-criteria decision selection (MCDS) framework was applied to rank all 24 configurations jointly. MCDS scores range from 0 to 1; higher scores indicate stronger integrated performance. The overall ranking results are presented in Figure 12. The following indicators were treated as lower-is-better criteria: air temperature, operative temperature, PPD, discomfort hours, heating demand, and cooling demand. PMV was evaluated based on proximity to thermal neutrality (target t\u2009=\u20090).

As shown in Figure 12, L-type configurations demonstrated the strongest overall performance. L27 achieved the highest composite MCDS score overall, reflecting the lowest operative temperature and discomfort hours in the study, alongside the lowest heating and cooling demand in the L family. This was followed by L22, L18, and L13, consistent with their comparatively low operative temperatures and PPD values.

In the next tier, U10 and U13 benefited from the lowest operative temperatures across all configurations (22.02 and 22.15°C), though their high cooling demand (739 and 947 kWh, respectively) moderated their overall scores. L15 offered a favorable balance of comfort and low energy demand. Box27 was the strongest courtyard configuration, achieving a competitive operative temperature of 22.58°C.

The remaining configurations scored between 0.62 and 0.77, reflecting the trade-off between thermal comfort performance and energy demand. II-type configurations generally ranked in the lower half of their comfort tier due to higher operative temperatures and discomfort hours. II27 (0.095) performed poorly across all indicators, with severe overheating confirmed by a PMV of 1.04 and 236 annual discomfort hours.

The overarching pattern across families is that morphological compactness and orientation jointly govern thermal performance. More open configurations with favorable self-shading and airflow distribution (particularly L-type) achieved lower operative temperatures and lower energy demand simultaneously, as illustrated in Figure 13.

Energy demand proved to be an important differentiator across families. As shown in Figure 13, L-type configurations recorded a total conditioning demand of 235–324 kWh, compared with 1,200–2,580 kWh for U-type, 2,075–2,485 kWh for Box-type, and 1,450–2,760 kWh for II-type. This four-to-ten-fold difference reflects the combined effect of morphology on solar gain, natural ventilation, and envelope exposure, and represents a critical consideration for post-war reconstruction where energy infrastructure is constrained.

Overall, L-type configurations achieved the highest composite scores owing to their balance of low operative temperatures, moderate discomfort hours, and substantially lower energy demand than all other families. The distribution of operative temperature and energy demand across all families is illustrated in Figures 12 and 13.

Rank	Config.	Air Temp (w = 0.10)	Operative T. (w = 0.25)	Heating D. (w = 0.075) (lower = better)	PPD (w = 0.15) (lower = better)	Discomfort H. (w = 0.25) (lower = better)	PMV (neutral) (closer to 0 = better)	Cooling D. (w = 0.075) (lower = better)	MCDS Composite Score
1	★ L27	1.00	1.00	0.88	1.00	1.00	1.00	0.88	**0.914**
2	L22	0.55	0.63	0.73	0.79	0.79	0.61	0.76	**0.830**
3	L18	0.37	0.56	0.85	0.76	0.78	0.58	0.72	**0.817**
4	L13	0.72	0.53	0.86	0.74	0.79	0.55	0.83	**0.812**
5	U10	0.68	0.49	0.52	0.66	0.66	0.52	0.53	**0.775**
6	U15	0.63	0.50	0.54	0.67	0.65	0.53	0.61	**0.775**
7	box27	0.57	0.90	0.45	0.88	0.77	0.63	0.59	**0.775**
8	L15	0.57	0.37	0.55	0.68	0.73	0.46	0.61	**0.768**
9	U27	0.53	0.82	0.51	0.82	0.70	0.66	0.66	**0.766**
10	U22	0.53	0.78	0.56	0.73	0.61	0.62	0.62	**0.755**
...	...	...	...	...	...	...	...	...	...
20	II13	0.52	0.63	0.54	0.56	0.41	0.53	0.61	**0.635**
21	II10	0.67	0.50	0.50	0.51	0.36	0.46	0.60	**0.593**
22	II15	0.53	0.48	0.50	0.47	0.35	0.44	0.59	**0.584**
23	box10	0.53	0.48	0.50	0.47	0.35	0.44	0.59	**0.584**
24	△ II27	0.00	0.00	0.35	0.00	0.00	0.42	0.30	**0.095**

Note: All indicators are normalised (0–1). Higher values are better for all criteria except Heating D., PPD, Discomfort H., and Cooling D., where lower values are better.

0.75 – 1.00
0.50 – 0.75
0.25 – 0.50
0.00 – 0.25

★ Best configuration (highest MCDS score)
△ Worst configuration (lowest MCDS score)

Figure 12. Multi-criteria performance ranking of all configurations based on normalized scores (0–1) and composite MCDS values. (Developed by the Authors).

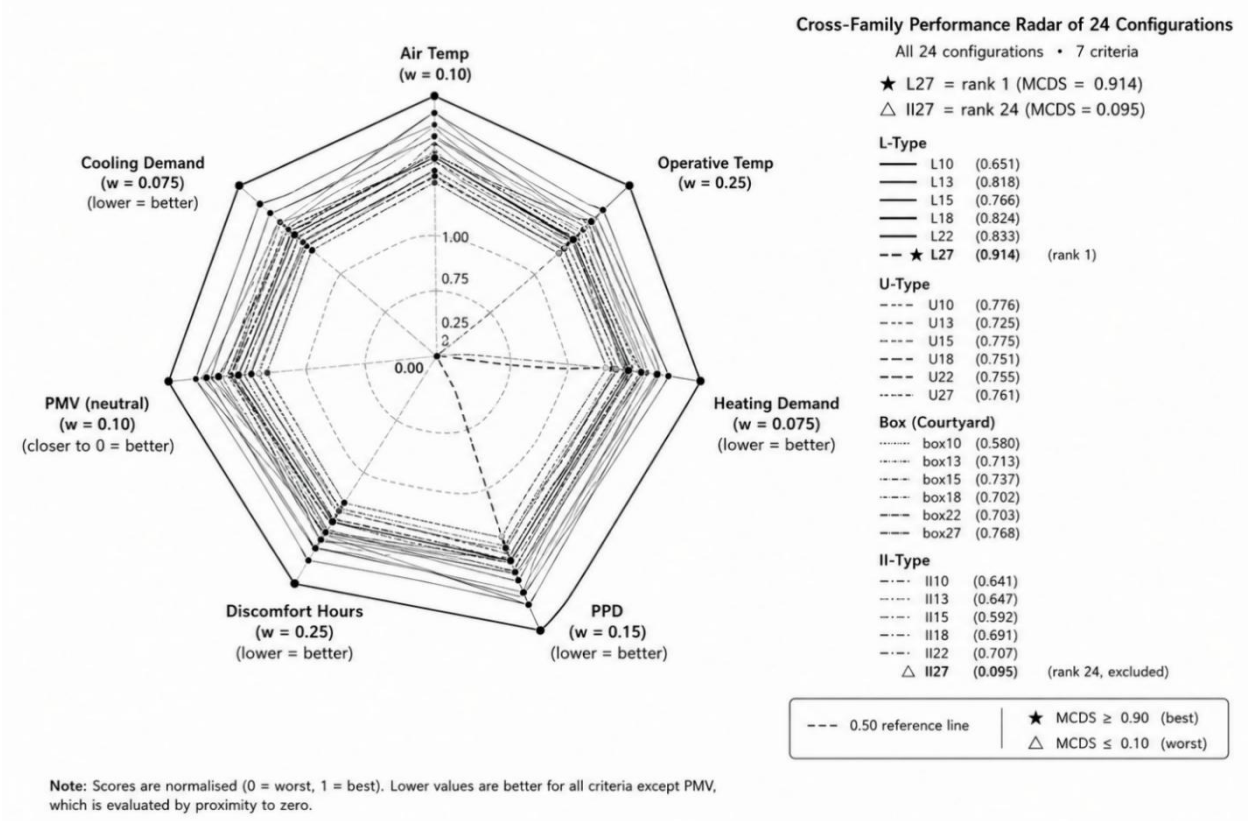

Figure 13. Cross-family radar comparison of normalised performance criteria illustrating trade-offs between thermal comfort and energy demand across morphological families. (Developed by the Authors).

4. Discussion

Simulation results from 24 residential configurations showed that building configuration and form demonstrably influence indoor thermal comfort, independent of mechanical conditioning, which was excluded from the simulation scope. These simulation results are consistent with previous studies (Trepci & Rodriguez-Ubinas, 2025; Elshafei et al., 2022) that investigated passive design in comparable hot-arid climates. These results examined seven performance indicators related to thermal comfort and energy demand, rather than relying on a single criterion. However, building configuration and form remained the primary dominant factor in thermal performance.

L-type configurations, particularly L27, received the strongest overall performance. This result reflects a clear physical mechanism. Within the L family, the open-angle plan geometry promotes self-shading on south- and west-facing walls and channels prevailing winds for passive airflow circulation and nocturnal heat dissipation, demonstrating how geometric organisation can offset the thermal penalties typically associated with higher exposed-envelope ratios in hot–arid climates. In Aleppo's summer conditions, where solar irradiance on south- and west-facing walls is intense and outdoor temperatures regularly exceed 40°C, this combination of controlled ventilation and partial self-shading suppresses peak operative temperatures during occupied hours, minimising cumulative discomfort hours and PMV deviation from neutrality.

Consequently, this combination of geometry, orientation, and self-shading explains why L-type configurations occupy the top four positions in the MCDS global rankings. This suggests that geometric airflow organization and self-shading effects can outweigh the thermal penalty typically associated with increased envelope exposure under specific hot–arid morphological conditions.

This finding reinforces the results of Zahiri and Altan (2016), who demonstrated that strategic façade shading significantly reduces thermal discomfort in comparable climates. The present study extends this observation across six A/V ratio variants within each family, providing a systematic morphological basis for the guidance rather than relying on a single building configuration.

Regarding the box-like form prevalent in local architecture within the studied climate, this study produced findings of particular relevance. Box 27 achieved competitive thermal performance, approaching the best designs in Group L, with an operative temperature of 22.58°C and PPD of 18.28%. This aligns with findings in comparable hot-arid climates demonstrating the efficiency of enclosed courtyards (Salkini, Greco, et al., 2017; Akande, 2010). Both studies documented the courtyard's ability to reduce the exposure of interior facades to sunlight, provide shade, and enhance natural ventilation pathways during the cooler nighttime hours.

However, previous studies comparing courtyard typologies did not fully account for the energy implications of enclosed morphologies. Box27 achieved a competitive operative temperature (22.58°C) and PPD (18.28%), comparable to the best L-type configurations. However, its cooling demand remained substantially higher than that of L27, reflecting the enclosed courtyard's greater solar gain absorption and reduced passive heat dissipation under hot–arid conditions. In a

post-war context where energy supply is constrained, this energy cost is a critical practical consideration alongside the comfort advantage.

The U-type building group exhibited behavior that differed from that reported in passive design studies for hot and dry regions. As the area-to-volume ratio increased (i.e., as the design density increased), thermal comfort indices improved significantly, but cooling demand rose sharply. The lower-A/V U-type configurations (U10 and U13) achieved the best MCDS scores in the family owing to their very low operative temperatures (22.02 and 22.15°C) alongside substantially lower cooling demand compared with the higher-A/V variants.

This pattern reflects the compound effect of A/V ratio on both thermal exchange and energy demand: as U-type configurations become more compact, cooling demand rises sharply (from 739 kWh at U10 to 1,977 kWh at U27), even as operative temperature remains nearly constant across the family (22.02–22.10°C). This decoupling of comfort and energy performance underscores the importance of including energy indicators alongside comfort metrics in morphological evaluation.

The design of building II27 differed significantly from all other designs, achieving the lowest MCDS score (0.095) at an A/V ratio of 1.00 m^{-1}. Its plan geometry creates a narrow passage between the two wings, accelerating airflow through the central corridor and increasing hot-air ingress during peak summer conditions. This behaviour contributes to elevated operative temperatures and persistent overheating under passive operation. On hot, dry days, the building is constantly exposed to an influx of outdoor air that can exceed 40°C at peak hours, raising rather than lowering indoor operative temperatures. This is confirmed by a PMV of 1.04—indicating severe warm discomfort conditions relative to the remaining configurations, the only configuration in the study to exceed the "Warm" threshold—and a PPD of 44.59%, with 236 annual discomfort hours. Consequently, occupants experience persistent thermal stress driven by excessive ingress of hot outside air. At A/V = 1.00 m^{-1}, aerodynamic amplification reaches its most severe expression in the II-form, producing the worst thermal performance across the entire study.

This result has direct design implications: double-wing configurations at high A/V ratios should not be used in hot, dry regions unless the passage between the wings is screened by solid courtyard walls or oriented away from prevailing hot winds.

Taken together, these results support a morphological hierarchy for the reconstruction of Aleppo. The study recommends the L-shape as the primary morphology for reconstruction, given its demonstrated advantage in both thermal comfort and energy demand. The courtyard (box) form remains architecturally and culturally appropriate for Aleppo (Kousa et al., 2021; Chambers, 2022), and its comfort performance is competitive, though its higher conditioning energy demand must be addressed through passive solar control and envelope design. The U-shape offers a viable compromise where a full courtyard enclosure is not feasible. The II-shape at high A/V ratios should be avoided unless the wind-corridor effect between the wings can be controlled through screening or orientation adjustment.

5. Conclusions

This study evaluated 24 residential morphologies across four plan families and six A/V ratio levels under Aleppo's current hot-arid climate, using a transparent multi-criteria framework grounded in ASHRAE 55 and ISO 7730. Heating and cooling energy demand were reported alongside comfort indicators, and the results establish a consistent morphological hierarchy for passive housing reconstruction, with the following evidence-based recommendations for designers and planners.

The results support the following evidence-based recommendations for designers and planners:

- Prioritize L-type compact designs for housing reconstruction. L27 or L22 are recommended as primary options for their strong thermal comfort performance and lowest energy demand in the study; L13 offers the best balance where energy minimisation is the primary constraint.
- Maintain courtyard architecture as a popular local design strategy, as both Box15 and Box27 outperformed most Type II and U alternatives, underscoring the continued relevance of the courtyard pattern in a post-war context.
- Avoid the II27 configuration: it exhibits severe overheating conditions (PMV = 1.04, operative temperature 25.63°C) and the highest energy demand (2,760 kWh total) in the study. Box 10 should also be avoided within the courtyard family due to the highest operative temperature (23.20°C) and discomfort hours (200) in its group.
- Account for energy demand in morphological selection: L-type configurations recorded total conditioning demand of 235–324 kWh, compared with 1,200–2,580 kWh for U-type, 2,075–2,485 kWh for Box-type, and 1,448–2,760 kWh for II-type—a four-to-ten-fold difference that is decisive in the resource-constrained post-war context.

These findings demonstrate that the morphology family and A/V ratio jointly exert a significant influence on both thermal comfort and energy performance, highlighting the importance of morphology-based design decisions in post-war residential reconstruction. Future research should pursue: (i) testing all 24 configurations against mid- to late-century climate projections (Meteonorm SSP2-4.5 and SSP5-8.5 scenarios) to evaluate ranking stability under projected warming; (ii) determining the energy savings achievable through the highest-rated morphologies under mixed passive–mechanical conditioning strategies; (iii) conducting formal sensitivity analysis to evaluate ranking robustness under alternative MCDS weighting assumptions; and (iv) integrating construction costs, operational energy savings, and community-memory values into a comprehensive reconstruction decision framework. The novelty of this research lies in the integrated evaluation of four residential morphology families across six A/V ratio levels using seven thermal-comfort and energy-performance indicators within a unified MCDS framework. This study contributes to the literature by providing a systematic comparison of residential morphologies under Aleppo's hot-dry Mediterranean climate. The proposed MCDS approach provides a practical decision-support tool for architects and planners involved in post-war reconstruction projects in Aleppo and similar climatic contexts.

Acknowledgements
The authors thank the academic supervisors and colleagues who provided feedback during the development of this study.

Funding
This research received no external funding.

Conflicts of Interest
The authors declare no conflict of interest.

Data Availability Statement
The simulation inputs and processed outputs supporting the findings of this study are available from the corresponding author upon reasonable request.

Institutional Review Board Statement
Not applicable.

CRediT Author Statement
Mariam Altaema: Conceptualisation; Data curation; Formal analysis; Investigation; Methodology; Visualisation; Writing – original draft; Writing – review & editing. Sertaç Oruç: Conceptualisation; Funding acquisition; Project administration; Resources; Supervision; Validation; Writing – review & editing. All authors have read and approved the final manuscript.

References

Akande, O. K. (2010). Passive design strategies for residential buildings in a hot, dry climate in Nigeria. WIT Transactions on Ecology and the Environment, 128, 61–70. https://doi.org/10.2495/ARC100061

Alazzy, A., Lü, H., & Zhu, Y. (2014). Impact of climate change on the evaluation of future water demand in the Euphrates and Aleppo basin, Syria. Proceedings of the International Association of Hydrological Sciences, 364, 307–312. https://doi.org/10.5194/piahs-364-307-2014

American Society of Heating, Refrigerating, and Air-Conditioning Engineers. (2020). ANSI/ASHRAE Standard 55-2020: Thermal environmental conditions for human occupancy. ASHRAE.

Atmaca, A., Gedik, G., & Wagner, A. (2021). Determination of optimum envelope of religious buildings in terms of thermal comfort and energy consumption: Mosque cases. Energies, 14(20), 6597. https://doi.org/10.3390/en14206597

Beck, H. E., Zimmermann, N. E., McVicar, T. R., Vergopolan, N., Berg, A., & Wood, E. F. (2018). Present and future Köppen-Geiger climate classification maps at 1-km resolution. Scientific Data, 5, 180214. https://doi.org/10.1038/sdata.2018.214

Aşıkoğlu Metehan, A., Şahin, A. S., & Biyıkoğlu, M. (2025). Adapting to climate change: Assessing future residential energy demand and resilience strategies in Türkiye through simulation-based building performance analysis. Buildings, 15(8), 1255. https://doi.org/10.3390/buildings15081255

Ben Ratmia, F. Z., Ahriz, A., Santi, G., Bouzaher, S., Mahar, W. A., Ben Ratmia, M. A. E., & Matallah, M. E. (2024). Street design strategies based on spatial configurations and building external envelopes in relation to outdoor thermal comfort in arid climates. Sustainability, 16(1), 221. https://doi.org/10.3390/su16010221

Chambers, K. (2022). RECONSTRUCTION OF ALEPPO, SYRIA: A DESIGN STUDIO AT THE UNIVERSITY OF NOTRE DAME, USA. In C. A. Brebbia (Ed.), Islamic Heritage Architecture IV (pp. 149–160). WIT Press. https://doi.org/10.2495/IHA220131

Delannoy, L., Puri, S., Perera, A. T. D., Coccolo, S., Mauree, D., & Scartezzini, J.-L. (2018). Climate impact and energy sustainability of future European neighborhoods. In the 2018 International Conference on Environment and Electrical Engineering and 2018 IEEE Industrial and Commercial Power Systems Europe (EEEIC / I&CPS Europe) (pp. 1–6). https://doi.org/10.1109/EEEIC.2018.8617066

DesignBuilder Software Ltd. (2021). DesignBuilder simulation software (Version 6.1.7.007) [Software].

Dirks, J. A., Gorrissen, W. J., Hathaway, J. H., Skorski, D. C., Scott, M. J., Pulsipher, T. C., Huang, M., Liu, Y., & Rice, J. S. (2015). Impacts of climate change on energy consumption and peak demand in buildings: A detailed regional approach. Energy, 79, 20–32. https://doi.org/10.1016/j.energy.2014.08.081

Elshafei, G., Katunský, D., Zeleňáková, M., & Negm, A. (2022). Green building outdoor thermal comfort in a hot desert climatic region. Cogent Engineering, 9(1), 2046681. https://doi.org/10.1080/23311916.2022.2046681

Erdemir Kocagil, İ., & Koçlar Oral, G. (2015). The effect of building form and settlement texture on energy efficiency for the hot dry climate zone in Turkey. Energy Procedia, 83, 98–107. https://doi.org/10.1016/j.egypro.2015.11.325

Escandón, R., Calama-González, C., Alonso, A., Suárez, R., & Rodríguez, Á. (2023). How do different methods for generating future weather data affect building performance simulations? A comparative analysis of southern Europe. Buildings, 13(9), 2385. https://doi.org/10.3390/buildings13092385

Ferdyn-Grygierek, J., Sarna, I., & Grygierek, K. (2021). Future climatic conditions and overheating risk in residential buildings in Central Europe. Sustainable Cities and Society, 65, 102628. https://doi.org/10.1016/j.scs.2020.102628

Ghadanfar, S. (2021, November 8–11). The role of urban resilience strategies in the economic recovery of post-conflict Aleppo: Enhancing livelihoods of the host, returnee, and displaced communities [Conference paper]. 57th ISOCARP World Planning Congress, Doha, Qatar.

Iles, S. M., Seddiki, M., & Kadi, L. (2023). Passivhaus and EnerPHit in the Mediterranean climate. International Journal of Sustainable Building Technology and Urban Development, 14(2), 169–190. https://doi.org/10.22712/susb.20230014

Intergovernmental Panel on Climate Change. (2021). Climate change 2021: The physical science basis. Contribution of Working Group I to the Sixth Assessment Report of the Intergovernmental Panel on Climate Change (V. Masson-Delmotte et al., Eds.). Cambridge University Press. https://doi.org/10.1017/9781009157896

International Organization for Standardization. (2005). ISO 7730: Ergonomics of the thermal environment — Analytical determination and interpretation of thermal comfort using calculation of the PMV and PPD indices and local thermal comfort criteria. ISO.

Isinkaralar, O., Sharifi, A., & Isinkaralar, K. (2024). Assessing spatial thermal comfort and adaptation measures for the Antalya basin under climate change scenarios. Climatic Change, 177(8), 118. https://doi.org/10.1007/s10584-024-03781-8

Jafarpur, P., & Berardi, U. (2021). Effects of climate change on building energy demand and thermal comfort in Canadian office buildings adopting different temperature setpoints. Journal of Building Engineering, 42, 102725. https://doi.org/10.1016/j.jobe.2021.102725

Khaddour, L. A. (2024). Comparative analysis of residential building envelopes newly implementing the building insulation code in Damascus. International Journal of Environmental Science and Technology, 21, 1509–1536. https://doi.org/10.1007/s13762-023-05053-x

Khatibi, A., & Krauter, S. (2021). Validation and performance of satellite meteorological dataset MERRA-2 for solar and wind applications. Energies, 14(4), 882. https://doi.org/10.3390/en14040882

Kousa, C., Pottgiesser, U., & Lubelli, B. (2021). Residential heritage transformations: How the architecture of Aleppo's courtyard houses has changed. Sustainability, 13(22), 12596. https://doi.org/10.3390/su132212596

Kutty, N. A., Barakat, D., Darsaleh, A. O., & Kim, Y. K. (2024). A systematic review of climate change implications on building energy consumption: Impacts and adaptation measures in hot urban desert climates. Buildings, 14(1), 13. https://doi.org/10.3390/buildings14010013

Lachheb, M., Younsi, Z., Youssef, N., & Bouadila, S. (2024). Enhancing building energy efficiency and thermal performance with PCM-integrated brick walls: A comprehensive review. Building and Environment, 256, 111476. https://doi.org/10.1016/j.buildenv.2023.111476

Ma, X., Chau, C. K., Lu, S., Leung, T. M., & Li, H. (2024). Modelling the effects of neighbourhood and street geometry on pedestrian thermal comfort in Hong Kong. Architectural Science Review, 1–16. https://doi.org/10.1080/00038628.2024.2391518

Meteotest AG. (2021). Meteonorm version 8.0: Global meteorological database for engineering and education [Software]. Meteotest AG.

Naaouf, E., & Torma, M. (2023). Climate of Syria based on CORDEX simulations: Present and future. Atmosphere, 14(8), 1235. https://doi.org/10.3390/atmos14081235

Peel, M. C., Finlayson, B. L., & McMahon, T. A. (2007). Updated world map of the Köppen–Geiger climate classification. Hydrology and Earth System Sciences, 11(5), 1633–1644. https://doi.org/10.5194/hess-11-1633-2007

Pham, M. T., Phap, V. T., Trung, N. D., Son, T. N., Kien, D. T., & Tho, V. V. (2022). A study on the impact of various meteorological data on the design performance of rooftop solar power projects in Vietnam: A case study of Electric Power University. Energies, 15(19), 7149. https://doi.org/10.3390/en15197149

Roetzel, A., Tsangrassoulis, A., & Dietrich, U. (2014). Impact of building design and occupancy on office comfort and energy performance in different climates. Building and Environment, 71, 165–175. https://doi.org/10.1016/j.buildenv.2013.10.001

Saaty, T. L. (1977). A scaling method for priorities in hierarchical structures. Journal of Mathematical Psychology, 15(3), 234–281. https://doi.org/10.1016/0022-2496(77)90033-5

Saaty, T. L. (1980). The analytic hierarchy process: Planning, priority setting, resource allocation. McGraw–Hill.

Salkini, H., Swaid, B., Greco, L., & Lucente, R. (2017). Emerging an adaptive kinetic mashrabia for reviving the environmental responsiveness in the traditional courtyard house of Aleppo. In Proceedings of the 35th International Conference on Education and Research in Computer Aided Architectural Design in Europe (eCAADe) (Vol. 1, pp. 299–308). https://doi.org/10.52842/CONF.ECAADE.2017.1.299

Salkini, H., Greco, L., & Lucente, R. (2017). Towards adaptive residential buildings: Traditional and contemporary scenarios in bioclimatic design (the case of Aleppo). Procedia Engineering, 180, 1083–1092. https://doi.org/10.1016/j.proeng.2017.04.268

Tang, H., Liu, J., & Zheng, B. (2022). Study on the green space patterns and microclimate simulation in typical urban blocks in central China. Sustainability, 14(22), 15391. https://doi.org/10.3390/su142215391

Tootkaboni, M., Ballarini, I., Zinzi, M., & Corrado, V. (2021). A comparative analysis of different future weather data for building energy performance simulation. Climate, 9(2), 37. https://doi.org/10.3390/cli9020037

Trepci, E., & Rodriguez-Ubinas, E. (2025). Passive design for residential buildings in arid desert climates: Insights from the Solar Decathlon Middle East. Buildings, 15(15), 2731. https://doi.org/10.3390/buildings15152731

Zahiri, S., & Altan, H. (2016). The effect of passive design strategies on thermal performance of female secondary school buildings during the warm season in a hot and dry climate. Frontiers in Built Environment, 2, 3. https://doi.org/10.3389/fbuil.2016.00003